

ANALYSIS AND IMPLICATIONS OF THE EDGE STRUCTURE OF DIOCTAHEDRAL PHYLLOSILICATES

G. NORMAN WHITE AND L. W. ZELAZNY

Department of Agronomy
Virginia Polytechnic Institute and State University
Blacksburg, Virginia 24061

Abstract—Crystal growth theory was applied to describe edge sites of phyllosilicates. Three face configurations were found to exist. One face has one tetrahedral site per tetrahedral sheet and two octahedral one-coordinated sites per crystallographic area $ac \sin \beta$, where a and c are layer dimensions and β is the angle between them. The other two faces are similar except that they have one less octahedral site which is replaced by one $\text{Si}^{\text{IV}}\text{—O—Al}^{\text{VI}}$ site in this same $ac \sin \beta$ area. A transfer of bonding energy from the remaining octahedral site to the $\text{Si}^{\text{IV}}\text{—O—Al}^{\text{VI}}$ site is believed to neutralize all edge charge on faces containing these latter sites at normally encountered pHs (pH 3–9). A similar charge rearrangement along the edges results in an apparent decrease in the permanent charge of the mineral with an increase in edge area.

On the basis of such an analysis, lath-shaped illite can be described as a very fine grained dioctahedral mica in which the apparent deficient occupancy of the octahedral sheet, presence of excess water, and measurable cation-exchange capacity may in part be the result of a large ratio of edge area to total volume, with no other chemical or structural change in the mica layers. The increasing importance of edge charge relative to layer charge produces erroneous formulae for 2:1 phyllosilicates in very fine grained samples containing fewer than 2 of 3 octahedral sites occupied by cations, on the basis of a 22-charge half cell.

Key Words—Celadonite, Edge structure, Illite, Muscovite, Octahedral site, Phengite.

INTRODUCTION

Most natural surfaces are charged to some degree. Surface charge arises from the lack of sufficient structural bonds to compensate completely for the charge from surface oxygens. Among common minerals, only the basal surfaces of some phyllosilicates and oxyhydroxides are of such a structure as to be wholly uncharged. All crystal surfaces of quartz and feldspars and some faces of phyllosilicates and oxyhydroxides possess a charge arising from broken bonds. Surface charge is the principal source of cation- and anion-retention characteristics of these minerals, whereas both surface and edge charge affect their rheological and specific adsorption properties.

To date, two models have been proposed to explain edge-charge characteristics of 1:1 dioctahedral phyllosilicates. These two models (Figure 1) have been extensively used to explain cation- and anion-retention properties of kaolinite, but the models have not been applied to other dioctahedral phyllosilicates. The earlier of the models is that of Schofield and Samson (1953), in which the edge of kaolinite is proposed to consist of three types of sites: octahedral Al—OH, tetrahedral Si—OH, and transitional tetrahedral-octahedral $\text{Si}^{\text{IV}}\text{—O—Al}^{\text{VI}}$ sites (Figure 1). At acid pHs, octahedral Al and tetrahedral Si are coordinated to water groups and the transitional site is hydroxylated, yielding a net charge of 1+. At moderate pHs, the octahedral group loses a proton to reduce the net charge to zero. At alkaline pHs, all adsorbed protons are removed, resulting in a net charge of 2−. Jackson (1964) pro-

posed a pK of 5.0 for the octahedral proton loss and a pK of 9.5 for the Si—OH deprotonation, with the transitional site having a pK somewhere in between.

The later model by Muljadi *et al.* (1966) differs from that of Schofield and Samson (1953) by the presence of two octahedral sites instead of one and no transitional sites (Figure 1). The charge shifts from one of the two octahedral sites to the other, giving the site an integral charge.

Neither model has gained universal acceptance, nor has either model been adjusted so as to be applicable to all phyllosilicates. In the present paper, a model based on crystal growth theory is proposed which can be used to determine the structure of the dominant crystal faces of any mineral. The model will be applied to the derivation of edge-charge characteristics of dioctahedral phyllosilicates. The consequences of the model on the 22-charge half-cell basis for formula calculation and the observed properties of illite and montmorillonite will also be examined.

THEORY

The stability of very small mineral particles (fine clay size) is highly dependent on their surface free energy (Berner, 1971). The importance of surface free energy on mineral stability is so strong for high surface-area solids that it has been proposed as a mechanism for the apparent reversal in the stabilities of some iron oxides (Langmuir and Whittemore, 1971). Two methods are commonly used to reduce the surface free energy of high surface-area solids. The first involves a

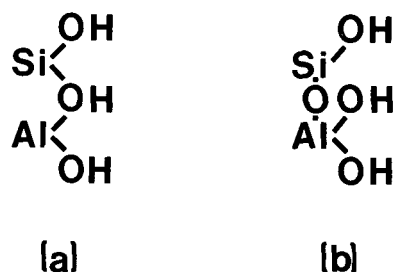


Figure 1. Schematic representation of the edge-site morphologies for kaolinite according to the models of (a) Schofield and Samson (1953) and (b) Muljadi *et al.* (1966).

rearrangement of the bond lengths and thereby bond strengths of surface sites and results in a decrease of surface charge. An example of this type of rearrangement occurs in palygorskite and sepiolite (Preisinger, 1959). The edge octahedra in these minerals are distorted, thereby eliminating charge from octahedral edge sites. On interior octahedra, the Mg–O bond lengths of O coordinated to three Mg atoms and either Si or H are a uniform 2.12 Å, with a $\frac{1}{3}$ valence unit charge. At edges, these bond lengths are distorted to 2.00 or 2.25 Å. The bond length for the 2-coordinated edge Mg–O bond having the O coordinated to two Mg atoms and one Si shortens to 2.00 Å and increases in bond strength to $\frac{1}{2}$, whereas the 1-coordinated Mg–OH₂ edge site increases in bond length to 2.25 Å, reflecting a 0 valence bond strength. With two octahedral bonds each of 0.50 valence-unit bond strength on the edge site containing 0 coordinated octahedra and 1 tetrahedron, the transitional edge site is effectively neutralized. The Mg–OH₂ site having zero bond strength is the 1-coordinated octahedral site. Together, these bond shifts neutralize what would have been two charge sites. The second method of reducing surface free energy involves a reduction of the number of potential edge sites per area. This method is the basis for crystal growth theory.

According to Hartman (1963, 1973, 1978), all stable crystal faces are parallel to one or more continuous chains of strong bonds. The more crystallographically different bond chains present parallel to a crystal face, the more likely the occurrence of that face. All that is needed for the application of Hartman's method is the determination of the number and orientation of the bond chains in the structure. Extension of crystal growth theory to the description of edge-site morphology requires no other data, inasmuch as the edges of the bond chains are the edge sites for the mineral surface.

To apply the crystal growth theory of Hartman (1973) to the description of edge sites of dioctahedral phyllosilicates, the structure must first be described as a network of bond chains. The bond chains in phyllosilicates are along [100], [110], and [1 $\bar{1}$ 0] (Grim and Güven, 1978; Hartman, 1982), parallel to the three pseudo-hexagonal x -axes (Bailey, 1967). The possible

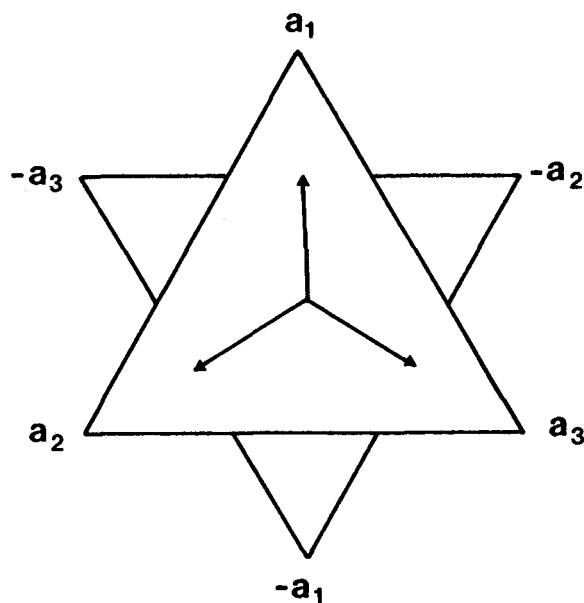


Figure 2. Idealized representation of the upper and lower faces of an octahedron showing the three possible x -axes.

structures of ideal dioctahedral phyllosilicate chains can be visualized by observing the basal surfaces of an octahedron (Figure 2). The three pseudo-hexagonal x -axes are perpendicular to the edges of the faces. The first tetrahedral sheet joins the top of the octahedral sheet at either a_1 , a_2 , or a_3 , which are symmetrically equivalent. If one tetrahedral sheet is attached, the three directions are no longer symmetrically equivalent, and the bottom tetrahedral sheet of a 2:1 phyllosilicate can only be joined at the site on the bottom of the octahedron related to the top site by a center of symmetry. Any other method of adding a second tetrahedral sheet results in a dipole. Three chain orientations result from joining the sheets in this manner. The three bond chains are not equivalent, but have one unique chain and two chains related by symmetry (Figure 3). The A, B, and C chains are observed along the a_3 , a_1 , and a_2 axes, respectively.

Crystal growth theory predicts that the building unit for crystal growth will have the same composition as the mineral itself. Neglecting exchangeable cations, the smallest growth unit for phyllosilicates (assuming congruent growth) should consist of one octahedron with one tetrahedron attached for each tetrahedral sheet (Figure 4). Larger multiples of this growth unit are required for minerals having ordered substitution. The orientation with which the growth unit attaches to the uncompleted bond chain is determined by the mineral's structure. The number and structure of the faces of ideal phyllosilicates can be described on the basis of the minimum repeat area $ac \sin \beta$, where a and c are the layer repeat dimensions and β is the angle between the [001] and [100]. The angle, β , only approximates

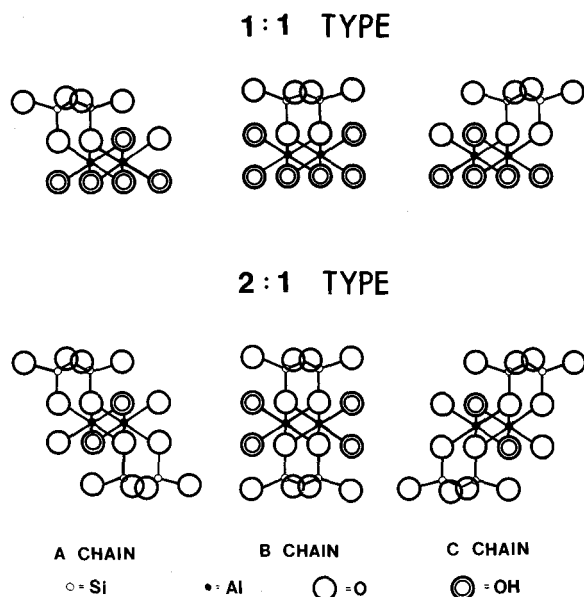


Figure 3. The three possible bond-chain morphologies for 1:1 and 2:1 phyllosilicates as viewed along the chain direction.

the angle in the structures of 1*Tc* pyrophyllite (Lee and Guggenheim, 1981) and 2*M₁* muscovite and phengite (Güven, 1980) but the error is less than 1% on a sine basis.

To derive the equilibrium structure of the faces as a function of pH, the octahedral-, transitional-, and tetrahedral-site pK values of Jackson (1964) were assumed, except at low pHs where a Si—OH₂⁺ group was added in accordance with the silica hydrolysis model of Stumm and Morgan (1981). The structure of the edges predicted by crystal growth theory have two different projections when viewed parallel to the bond chains (Figure 5), but do not differ when viewed perpendicular to the chains. The projections for chains A and C are equivalent and contain one tetrahedral site per tetrahedral sheet, one transitional octahedral-tet-

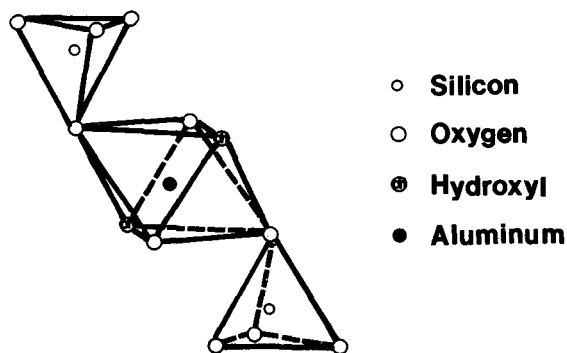


Figure 4. Representation of the minimum congruent crystal-growth unit for a phyllosilicate assuming no substitutional ordering.

rahedral site, and one 1-coordinated octahedral site per area $ac \sin \beta$. Chain B contains one tetrahedral site per tetrahedral sheet and two octahedral sites for the area $ac \sin \beta$ (Table 1). In any layer of a phyllosilicate, one edge face will be bound by one of the chains.

DISCUSSION

The edge-site morphologies predicted for kaolinite agree with the model of Schofield and Samson (1953) or the model of Muljadi *et al.* (1966), depending upon which crystal face is considered. The predicted morphology for edges bound by chains A and C agrees with that proposed by Schofield and Samson (1953), whereas that predicted for faces bound by chain B agrees with the Muljadi *et al.* (1966) model.

The advantage of using crystal growth theory for predicting edge-site morphology is that the model is three dimensional, allowing for calculation of the density of a site on a surface. The calculation of edge-charge characteristics for faces bound by chain B is straightforward (Table 1), but the presence of the transitional octahedral-tetrahedral sites on chains A and C make calculations more difficult. The transitional site

Table 1. Concentration of edge-charge sites on representative dioctahedral phyllosilicate faces.

Mineral	Composition	$ac \sin \beta$ (Å ²)	Bound by B chain ³				Bound by A or C chains ³						
			Oct. (sites/unit area)	Tet. (μmole/m ²)	Oct. (sites/unit area)	Tet. (μmole/m ²)	Oct.	Trans.	Tet.	Oct.	Trans.	Tet.	
Kaolinite	Al ₂ Si ₂ O ₅ (OH) ₄	36.63	2	1	9.07	4.53	0	0	1	0	0	0	4.53
Pyrophyllite	Al ₂ Si ₄ O ₁₀ (OH) ₂	47.46	2	2	7.00	7.00	0	0	2	0	0	0	7.00
Beidellite ¹	M _{0.33} Al ₂ (Si _{3.67} Al _{0.33})O ₁₀ (OH) ₂	51.80	2	1.92	6.41	6.14	0	0	1.92	0	0	0	6.14
Montmorillonite ¹	M _{0.33} (Al _{1.67} Mg _{0.33})Si ₄ O ₁₀ (OH) ₂	52.10	1.66	2	5.32	6.39	0	0	2	0	0	0	6.39
Vermiculite ²	M _{0.67} Al ₂ (Si _{3.33} Al _{0.67})O ₁₀ (OH) ₂	51.16	2	1.83	6.49	5.95	0	0	1.83	0	0	0	5.95
Muscovite	KAl ₂ (Si ₃ Al)O ₁₀ (OH) ₂	51.60	2	1.5	6.44	5.63	0	0	1.5	0	0	0	5.63
Celadonite	K(AlMg)Si ₄ O ₁₀ (OH) ₂	53.30	1	2	3.12	6.23	0	0	2	0	0	0	3.12

¹ Assumes $c = 10.0 \text{ \AA}$ and $\beta = 90^\circ$.

² Assumes $a = 5.154 \text{ \AA}$, $c = 10.0 \text{ \AA}$, and $\beta = 97^\circ$.

³ See text for definition of A, B, and C chains.

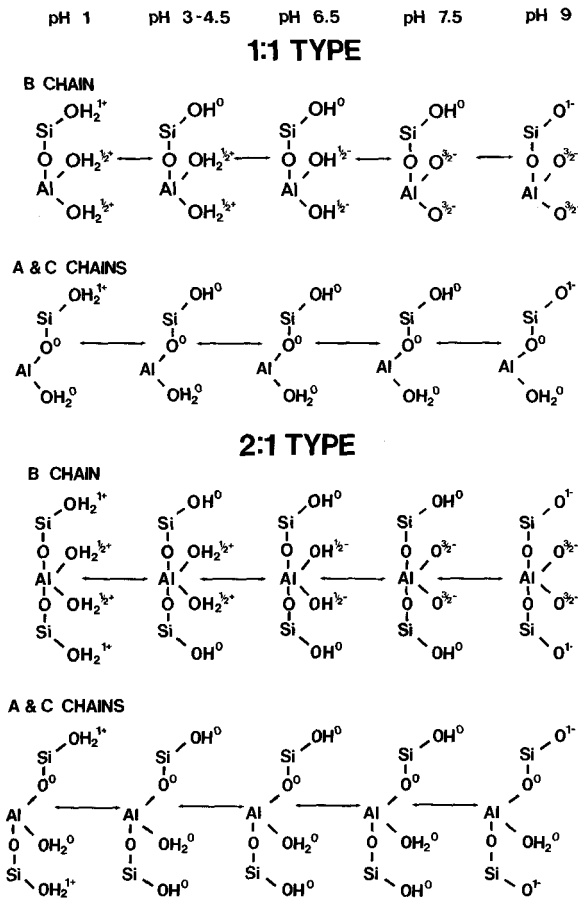


Figure 5. Effects of pH on the charge properties of the two proposed edge-site morphologies for dioctahedral phyllosilicates.

may possibly exist as a charge site, but it is also reasonable to hypothesize a shift in the octahedral cation. This shift would cause the bond length to shorten between the octahedral cation and the transitional site and increase the length of the bond to the octahedral edge site. Such a bond shift would cause the octahedral bond of the transitional site to increase in strength from 0 to 1, while removing all charge from the 1-coordinated site, thus resulting in a neutralization of the octahedral surface charge for these faces (Figure 6). Similar shifts have been reported in the crystal structure of sepiolite (Preisinger, 1959) and are an essential, although unstated part of the Muljadi *et al.* (1966) model. The tetrahedral site is charged at low and high pHs due to protonation and deprotonation of the site, respectively, but at common environmental pHs (pH 3–9) the surface is uncharged. If the shift of bond strength required for the minimization of surface charge does not occur, the Schofield and Samson (1953) model is adequate to describe the charge characteristics of these faces.

The edge sites in 2:1 dioctahedral phyllosilicates are

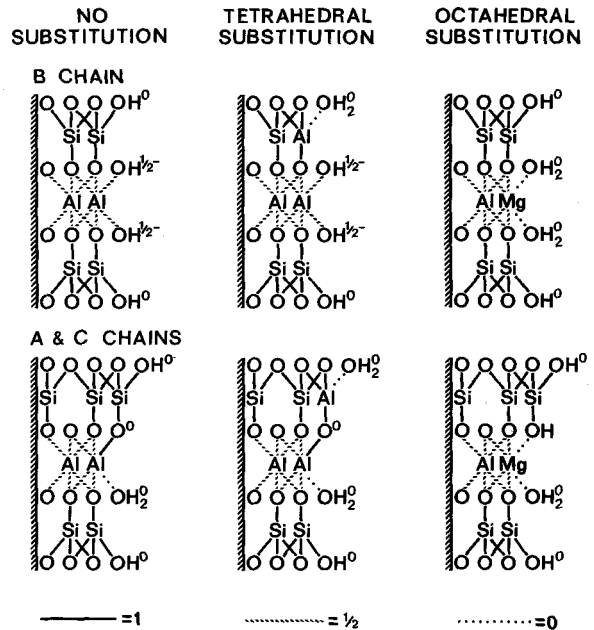


Figure 6. Effects of tetrahedral and octahedral substitution on bond strength and edge charge of the two proposed edge-site morphologies for 2:1 dioctahedral phyllosilicates at pH 6.5.

more complex structurally, but are chemically more complex only for minerals having significant octahedral and tetrahedral substitution. The addition of the second tetrahedral sheet adds one tetrahedral site per area $ac \sin \beta$ as compared to 1:1 phyllosilicates, but does not change the remainder of the edge charge. The result of substitution of Al for Si in the tetrahedral sheet is countered by a shift in bond strength from the ideal $3/4$ charge for each of four sites to a configuration in which the three interior bonds have a bond strength of one each, while the edge site becomes an uncharged bound water (Figure 6). A similar shift occurs in the octahedral sheet in sites where a divalent cation is present. The bonds from divalent cations would shift such that all charge would be removed from the octahedral edge sites and be shifted to the internal sites resulting in an increase of the bond strength from the ideal $1/2$ charge to $1/2$ charge. For B chains, the net result of a divalent octahedral cation substitution is a loss of all octahedral edge charge for sites with substitutions. On A and C chain edges, the transitional edge site would become an uncharged hydroxyl with the octahedral site becoming a bound water site. The decreased charge of faces bound by A and C chains relative to B chains causes these former faces to grow faster, resulting in decreased importance of these faces. It is also important to note that as a result of bond shifts on mineral edges, as the permanent charge of the phyllosilicate increases, edge (pH dependent) charge decreases on a structural $ac \sin \beta$ basis. In addition, the permanent

Table 2. Calculated water and apparent unit-cell water percentages for muscovite, phengite, and celadonite laths of $0.1 \times 0.01 \mu\text{m}$ size.

Mineral	Calculated total water (apparent unit-cell water) (%) ¹ at pHs of			
	1	3	6	9
Muscovite	7.00 (4.99)	6.63 (4.99)	6.13 (5.01)	5.63 (5.02)
Mg-phengite	7.01 (5.01)	6.58 (5.01)	6.20 (5.02)	5.83 (5.05)
Fe-phengite	6.72 (4.80)	6.30 (4.80)	5.94 (4.81)	5.59 (4.83)
Mg-celadonite	7.03 (5.01)	6.53 (5.01)	6.28 (5.02)	6.03 (5.04)
Fe-celadonite	6.52 (4.60)	6.06 (4.60)	5.83 (4.61)	5.60 (4.63)

¹ Calculated using the backbone weight basis for formulae as stated in Figure 1 and edge configurations as shown in Figure 5.

charge of phyllosilicates decreases near the edge due to these charge shifts.

The application of this model to phyllosilicates having more complex stacking is simplified by considering that the various polymorphs have ordered combinations of the edges predicted for $1M$ micas. This arrangement would involve the mixing of fast-growing A and C chains with slower growing B chains. For $2M_1$ muscovite, for example, the [100] edge would have a surface consisting of alternating A and C chains, whereas the faces paralleling [110] and [1 $\bar{1}$ 0] would alternate B chains with either A or C chains.

Particle size and morphology have large effects on the scale to which edge charge manifests itself. For each tenfold decrease in edge area, a tenfold increase in importance of the edge sites should be observed. As a result, particle edge sites are of stoichiometric importance for very thin lath morphologies, such as is common for illite, but not as important for larger pseudo-hexagonal kaolinite. The edge of laths are of stoichiometric importance if they are $0.01 \mu\text{m}$ wide (Tables 2 and 3), but an order of magnitude larger particle should not show any significant difference from ideal micas. For example, only 1 of 10 illite samples reported by Środoń *et al.* (1986) ($<5.0\text{-}\mu\text{m}$ size fractions) showed an octahedral layer having fewer than 2 of 3 sites filled (indicative of small particle size), whereas 12 of 23 sites of the $<0.125\text{-}$ or $<0.3\text{-}\mu\text{m}$ fractions showed this octahedral deficiency. Particle morphology

is also important. On a weight basis, a much greater edge area exists for pseudo-hexagonal morphologies than for lath morphologies having the same width. If the calculations are performed on an equal basal-area basis, the differences due to morphology are less significant.

The thickness of very fine clay particles is also important. The outer (001) surfaces of a particle is a source of permanent cation-exchange properties. These faces become important in the formula determination of clays when the thickness of the particle decreases. If a clay particle is considered to be n layers thick, there will be $n - 1$ internal surfaces and 1 external surface. It has been recently proposed that many illite/smectites may be true illites of only 2 or 3 layers, with the outer layers acting as the smectite (Nadeau *et al.*, 1984a, 1984b). In micas, internal surfaces are the source of fixed K, whereas external surfaces are the source of the observed permanent cation exchange. If external surfaces are a significant portion of the total internal and external surface area (i.e., the mica particles are thin along [001]), the material may have a significant CEC, even in the absence of smectite. In the structural half-cell formula of a thin mica platelet, $(n - 1)/n$ times the permanent charge is neutralized by internal K and $1/n$ times the permanent charge is neutralized by exchangeable cations on external (001) surfaces.

These surface effects may be stoichiometrically important in minerals having a large edge area, such as

Table 3. Calculated apparent unit-cell formulae for muscovite, phengite, and celadonite laths of $0.1 \times 0.01 \mu\text{m}$ size.

Mineral	pH	Apparent unit-cell structural formula ¹
Muscovite	<5	$\text{K}_{0.82}\text{Al}_{2.05}(\text{Si}_{3.03}\text{Al}_{0.97}\text{O}_{10}(\text{OH})_2)$
	5–8	$\text{M}^{+}_{0.26}\text{K}_{0.80}\text{Al}_2(\text{Si}_3\text{Al})\text{O}_{10}(\text{OH})_2$
	>8	$\text{M}^{+}_{0.30}\text{K}_{0.80}\text{Al}_{1.97}(\text{Si}_{2.99}\text{Al}_{1.01})\text{O}_{10}(\text{OH})_2$
Phengite	<5	$\text{K}_{0.82}(\text{Mg}, \text{Fe}^{2+})_{0.50}\text{Al}_{1.55}(\text{Si}_{3.53}\text{Al}_{0.47})\text{O}_{10}(\text{OH})_2$
	5–8	$\text{M}^{+}_{0.16}\text{K}_{0.80}(\text{Mg}, \text{Fe}^{2+})_{0.50}\text{Al}_{1.51}(\text{Si}_{3.51}\text{Al}_{0.49})\text{O}_{10}(\text{OH})_2$
	>8	$\text{M}^{+}_{0.45}\text{K}_{0.79}(\text{Mg}, \text{Fe}^{2+})_{0.49}\text{Al}_{1.44}(\text{Si}_{3.46}\text{Al}_{0.54})\text{O}_{10}(\text{OH})_2$
Celadonite	<5	$\text{K}_{0.79}(\text{Mg}, \text{Fe}^{2+})_{1.01}\text{Al}_{1.01}(\text{Si}_{4.04})\text{O}_{10}(\text{OH})_2$
	5–8	$\text{M}^{+}_{0.06}\text{K}_{0.80}(\text{Mg}, \text{Fe}^{2+})_{1.01}\text{Al}_{1.01}(\text{Si}_{4.02})\text{O}_{10}(\text{OH})_2$
	>8	$\text{M}^{+}_{0.28}\text{K}_{0.80}(\text{Mg}, \text{Fe}^{2+})_{1.00}\text{Al}_{0.98}(\text{Si}_{3.98}\text{Al}_{0.02})\text{O}_{10}(\text{OH})_2$

¹ Calculated using the backbone weight basis for formulae as stated in Figure 1 and edge configurations as shown in Figure 5. The edge charge is represented by M^{+} . Excess anions are neglected as if the result of a total elemental analysis.

lath-shaped illites. Güven *et al.* (1980) hypothesized that illite growth nuclei were 1M mica laths elongated along [100]. Electron microscopy showed these laths are commonly 0.01 μm or less in width. Type B chains parallel [100] in 1M micas. A particle of illite having such a morphology would have two edge areas, $ac \sin \beta$, per 10 to 12 unit cells. If the edge structure has pK values near those in the literature (summarized in Figure 5), very high water contents should be observed for otherwise ideal micas due to the edge contribution alone (Table 2). In addition, the charge of the edges would result in a breakdown of the 22-charge basis for the chemical formulae, resulting in fewer than 2 of 3 octahedral sites occupied by cations (Table 3). The calculated water contents and formulae for micas of this morphology and size suggest that the observed phengitic composition, excess water, octahedral site filling of less than 2 of 3 sites, and hypothesized montmorillonite layers are due to a breakdown in the method of formula calculation. Formulae for smectites, which are also typically fine size, have also been reported to have fewer than 2 of 3 octahedral sites filled (see, e.g., the Wyoming bentonite formulae in Weaver and Pollard, 1973).

SUMMARY AND CONCLUSIONS

Crystal growth theory can be applied to the determination of the equilibrium surface structure of minerals. The surface structure of each mineral face can be derived, but the proportions of the various faces cannot. Application of crystal growth theory to phyllosilicates predicts the morphology observed for phyllosilicates. A decrease in the number of edge sites per unit area is predicted to accompany an increase in permanent charge for phyllosilicates. As a result, the use of a 22-charge basis to produce a half unit-cell formula for 2:1 phyllosilicates may not be valid if the sample is chiefly very fine particle size. Illite characteristics may be explained as a result of small particle size of an otherwise normal dioctahedral mica.

REFERENCES

- Bailey, S. W. (1967) Polyttypism of layer silicates: in *AGI Short Course Lecture Notes on Layer Silicates*, S. W. Bailey, G. W. Brindley, W. D. Keller, D. R. Wones, and J. V. Smith, eds., Amer. Geol. Inst., Washington, D.C., SB1A-SB28A.
- Berner, R. A. (1971) *Principles of Chemical Sedimentology*: McGraw-Hill, New York, 240 pp.
- Grim, R. E. and Güven, N. (1978) *Bentonites: Geology, Mineralogy, Properties, and Uses*: Elsevier, New York, 256 pp.
- Güven, N. (1980) The crystal structures of 2M₁ phengite and muscovite: *Z. Kristallogr.* **134**, 196–212.
- Güven, N., Hower, W. F., and Davics, D. K. (1980) Nature of authigenic illites in sandstone reservoirs: *J. Sed. Petrol.* **50**, 761–766.
- Hartman, P. (1963) Structure, growth and morphology of crystals: *Z. Kristallogr.* **119**, 65–78.
- Hartman, P. (1973) Structure and morphology: in *Crystal Growth: An Introduction*, P. Hartman, ed., North-Holland Publ., Amsterdam, 367–402.
- Hartman, P. (1978) On the validity of the Donnay-Harker Law: *Can. Mineral.* **16**, 387–391.
- Hartman, P. (1982) On the growth of dolomite and kaolinite crystals: *N. Jb. Miner. Mh.* **1982**, 84–92.
- Jackson, M. L. (1964) Chemical composition of soils: in *Chemistry of the Soil*, F. E. Bear, ed., Reinhold, New York, 71–141.
- Langmuir, D. and Whitemore, D. O. (1971) Variations in the stability of precipitated ferric oxyhydroxides: in *Nonequilibrium Systems in Natural Water Chemistry*, R. F. Gould, ed., Adv. Chem. Ser. No. **106**, 209–234.
- Lee, J. H. and Guggenheim, S. (1981) Single crystal X-ray refinement of pyrophyllite-1Tc: *Amer. Mineral.* **66**, 350–357.
- Muljadi, D., Posner, A. M., and Quirk, J. P. (1966) The mechanism of phosphate adsorption by kaolinite, gibbsite, and pseudoboehmite: *J. Soil Sci.* **17**, 212–247.
- Nadeau, P. H., Tait, J. M., McHardy, W. J., and Wilson, M. J. (1984a) Interstratified XRD characteristics of physical mixtures of elementary clay particles: *Clay Miner.* **19**, 67–76.
- Nadeau, P. H., Wilson, M. J., McHardy, W. J., and Tait, J. M. (1984b) Interstratified clays as fundamental particles: *Science* **225**, 923–925.
- Preisinger, A. (1959) X-ray study of the structure of sepiolite: in *Clays and Clay Minerals, Proc. 6th Natl. Conf., Berkeley, California, 1957*, Ada Swineford, ed., Pergamon Press, New York, 61–67.
- Schofield, R. D. and Samson, H. R. (1953) The deflocculation of kaolinite suspensions and the accompanying change over from positive to negative chloride adsorption: *Clay Miner. Bull.* **2**, 45–51.
- Środoń, J., Morgan, D. J., Eslinger, E. V., Eberl, D. D., and Karlinger, M. R. (1986) Chemistry of illite/smectite and end-member illite: *Clays & Clay Minerals* **34**, 368–378.
- Stum, W. and Morgan, J. J. (1981) *Aquatic Chemistry*: John Wiley, New York, 780 pp.
- Weaver, C. E. and Pollard, L. D. (1973) *The Chemistry of Clay Minerals*: Elsevier, New York, 213 pp.

(Received 1 August 1986; accepted 6 August 1987; Ms. 1603)